Hutchinson, Claire V. and Ledgeway, Tim and Allen, Harriet A. and Long, Mike D. and Arena, Amanda (2013) Binocular summation of second-order global motion signals in human vision. Vision Research, 84 . pp. 16-25. ISSN 0042-6989

Binocular summation of second-order global motion signals in human vision

Claire V. Hutchinson[a*], Tim Ledgeway[b], Harriet A. Allen[b], Mike D. Long[a] , Amanda Arena[a]

[a] School of Psychology, College of Medicine, Biological Sciences and Psychology, University of Leicester, Lancaster Road, Leicester, UK

[b] School of Psychology, University of Nottingham, University Park, Nottingham, UK

*Contact details for corresponding author:
Tel: +44 (0) 116 2297183
E-mail: ch190@le.ac.uk

Running head: binocular summation of second-order global motion

Keywords: global motion, binocular summation, second-order, first-order

Abstract

Although many studies have examined the principles governing first-order global motion perception, the mechanisms that mediate second-order global motion perception remain unresolved. This study investigated the existence, nature and extent of the binocular advantage for encoding second-order (contrast-defined) global motion. Motion coherence thresholds (79.4 % correct) were assessed for determining the direction of radial, rotational and translational second-order motion trajectories as a function of local element modulation depth (contrast) under monocular and binocular viewing conditions. We found a binocular advantage for second-order global motion processing for all motion types. This advantage was mainly one of enhanced modulation sensitivity, rather than of motion-integration. However, compared to findings for first-order motion where the binocular advantage was in the region of a factor of around 1.7 [Hess et al., 2007, Vision Research 47, 1682-1692 & the present study], the binocular advantage for second-order global

motion was marginal, being in the region of around 1.2. This weak enhancement in sensitivity with binocular viewing is considerably less than would be predicted by conventional models of either probability summation or neural summation.

Introduction

Global motion perception refers to an individual's ability to combine the motion of individual local elements in a visual scene into a unified representation of overall image movement. Global motion signals are generated by the movement of objects in the world, by our own eye movements, and by our self-motion through space. Our capacity to encode global motion is fundamental to effectively navigating our way through the world in which we live. There is an abundance of evidence that the neural substrates underlying the extraction of global motion comprise a two-stage processing network involving striate (area V1) and extrastriate (areas MT & MST) cortices. Direction-selective neurons in V1 encode the direction of locally moving elements. This information is projected up-stream to motion-sensitive extrastriate visual areas such as areas MT and MST where receptive fields are much larger (Livingstone, Pack & Born, 2001) and integrate information from across the visual field (see Andersen, 1997 for a review). Firing rates of V1 neurons are strongly influenced by stimulus contrast, and typically exhibit a rapid initial rise followed by compression and saturation as the contrast level increases (e.g. Albrecht & Hamilton, 1982). However, neural responses in higher-order (extrastriate) visual areas typically saturate at much lower contrasts (e.g. Hall, Holliday, Hillebrand et al., 2005). Up to 90 % of MT neurons in the macaque are direction-selective (Albright, 1993), responding to motion that moves along translational axes (Movshon & Newsome, 1996). Lesions in MT lead to a range of selective deficits for the perception of motion such as significant reductions in the ability to discriminate global motion direction (Newsome & Paré, 1988), serious impairments of visual pursuit movement (Dürsteler & Wurtz, 1988) and deficits in motion and flicker perception (Schiller, 1993). In area MST, cells respond to even more complex features of a motion stimulus. Some neurons in area MST respond selectively to radial and circular motion (Duffy & Wurtz, 1991) such as expanding and contracting movements, rotations or even spiralling motions and are believed to be responsible for encoding the patterns of 'optic flow' generated by self-motion during visually-guided navigation (Grossberg, Mingolla & Pack, 1999).

There is evidence that binocularity is important in global motion perception. The ability to discriminate the direction of global motion is enhanced by binocular disparity (e.g. Hibbard & Bradshaw, 1999; Snowden & Rossiter, 1999; Greenwood & Edwards, 2006). In addition, conditions marked by deficits in binocular function, such as amblyopia, show deficits in global motion perception in the amblyopic and fellow fixing eyes, suggesting a deficit at a binocular locus (e.g. Giaschi, Regan, Kraft & Hong, 1992; Simmers, Ledgeway, Hess & McGraw, 2003). We have previously assessed the nature and extent of the binocular advantage for first-order (luminance-defined) global motion (Hess, Hutchinson, Ledgeway & Mansouri, 2007), using random dot kinematograms (RDKs) depicting either radial, rotational or translational flow fields. Motion coherence thresholds (% 'signal' dots required for reliable direction identification) were measured over a range of dot modulation depths (contrasts), under both monocular and binocular viewing. Thresholds initially decreased as the dot modulation depth increased, but performance became asymptotic at the highest contrasts tested for all types of motion. For binocular viewing the threshold versus dot modulation depth function was simply shifted laterally, along the x-axis towards lower contrasts, compared with the monocular function by about a factor of 1.7. So in this case the advantage of binocular viewing over monocular viewing was mediated by a process sensitive to image contrast, suggesting that the site of binocular combination for first-order motion perception occurs prior to the extrastriate cortex where global motion integration occurs.

The overwhelming majority of studies that have examined global motion perception have done so using first-order motion stimuli such as RDKs. However, like first-order RDKs, second-order (contrast-defined) RDKs can also provide a compelling impression of global motion. These patterns are defined by an ensemble of random dots, each of which modulates the contrast of a (first-order) carrier and movement is of the dots, not the carrier pattern (see figure 1 for an example of high contrast dots on a low contrast background). When dot modulation depth is high, second-order motion coherence thresholds can be a low as around 10 % of signal dots, similar to those observed for first-order global motion (Aaen-Stockdale, Ledgeway & Hess, 2007). However there are fundamental differences in the manner in which first-order motion and second-order motion are analysed. From a computational perspective

second-order motion patterns are likely to require more complex levels of analysis by the visual system than their first-order, luminance-defined, counterparts (e.g. Chubb & Sperling, 1988). Empirically there is a wealth of psychophysical evidence consistent with the notion that the two varieties of motion are encoded separately in the early stages of visual processing (for reviews see Baker, 1999; Lu & Sperling, 2001). Furthermore neurological evidence suggests that second-order motion processing relies on a network of distinct, and perhaps 'higher order' extrastriate brain areas (e.g. Greenlee & Smith, 1997; Vaina & Soloviev, 2004) than first-order motion perception, though the evidence from brain-imaging (fMRI) is more equivocal (Dumoulin, Baker, Hess & Evans, 2003; Nishida, Sasaki, Murakami, Watanabe & Tootell, 2003; Seifert, Somers, Dale & Tootell, 2003; Ashida, Lingnau, Wall & Smith, 2007).

Although first-order and second-order motion may be detected initially by separate mechanisms, it is also likely that, at some stage, their outputs are combined to compute the net direction of image motion. Visual area V5/MT has been put forward as the most likely cortical site of combination for first-order and second-order motion patterns (Wilson, Ferrera & Yo, 1992), a notion strengthened by evidence for "form-cue invariance" in primate area MT, where many neurons respond to both varieties of motion (Albright, 1987, 1992; Geesaman & Anderson, 1996; Churan & Ilg, 2001). However cue invariance has also been found in V1 (Chaudhuri & Albright, 1997), so the issue of exactly where this property originates in the visual system is complicated by the fact that there are many feedback connections from higher visual areas to those earlier in the visual pathways. Furthermore it has been claimed (e.g. Edwards & Badcock, 1995; Badcock & Khuu, 2001) that in human vision the pathways that process first-order motion and second-order motion remain separate up to, and including, the level at which global motion and optic flow analyses occur (i.e. V5/MT and MST), but some findings cast doubt on this assertion (e.g. Stoner & Albright, 1992; Mather & Murdoch, 1998). Consequently many of the precise properties of the mechanisms that mediate second-order global motion perception are still unresolved and require further investigation.

Although binocularity has been shown to be important in first-order global motion, the role of binocularity in the context of second-order global motion processing remains unclear. This study investigated a number of key issues concerning the binocular properties of the mechanisms that encode second-order global motion: (1) the extent and nature of any binocular advantage; and (2) the effect of global motion type (radial, rotational or translational motion) on second-order binocularity.

Methods

Observers

Six observers took part. Three were authors and three were naïve observers. All had normal or corrected-to-normal visual acuity and normal binocular vision.

Apparatus and stimuli

Stimuli were generated using a *Macintosh G4* computer and presented on a *Dell* monitor with an update rate of 75 Hz. The monitor was gamma-corrected with the aid of internal look-up tables. This was confirmed psychophysically (Ledgeway & Smith, 1994). The mean luminance of the display was 49 cd/m^2. Stimuli were presented within a circular window at the centre of the display that subtended 12 ° at the 92 cm viewing distance.

Global motion stimuli were either radial, rotational or translational second-order RDKs. 50 non-overlapping, second-order (contrast-modulated) dots were presented within a 12 ° diameter display aperture. This aperture contained a carrier composed of spatially 2-d, static, random visual noise in which individual pixel elements were assigned to be either ‘black’ or ‘white’ with equal probability. The noise had a Michelson contrast of 0.1 (before modulation by the dots, see below). The remainder of the screen was set to mean luminance.

Each RDK was generated anew immediately prior to its presentation and was composed of a sequence of 8 images, which when presented consecutively

produced continuous apparent motion. The duration of each image was 53.3 ms, resulting in a total stimulus duration of 426.7 ms. Dot density was 0.44 dots/deg^2 and the diameter of each dot was 0.235 °. At the beginning of each motion sequence, the position of each dot was randomly assigned. On subsequent frames, each dot was shifted by 0.3 °, resulting in a drift speed, if sustained, of 5.9 °/s. When a dot exceeded the edge of the circular display window it was immediately re-plotted in a random spatial position within the confines of the display aperture.

The modulation depth of the dots was manipulated by increasing the mean contrast of the noise carrier within the dots with respect to the mean contrast of the noise carrier in the background (c.f. Simmers et al., 2003). This was done using the following equation:

$$\text{Dot modulation depth} = (DC_{mean} - BC_{mean}) / (DC_{mean} + BC_{mean}), \quad [1]$$

where DC_{mean} and BC_{mean} are the mean contrasts of the carrier within the dots and background, respectively. Dot modulation varied in the range 0.35 to 0.8. A stimulus schematic is shown in Figure 1.

<Insert Figure 1 about here>

The global motion coherence level of the stimulus was manipulated by constraining a fixed proportion of ‘signal’ dots on each image update to move coherently along a trajectory (either radial, rotational or translational) and the remainder (‘noise’ dots) to move in random directions. For radial motion, on each trial signal dots were displaced along trajectories consistent with either expansion or contraction with equal probability. For rotational motion, signal dots rotated either clockwise or anti-clockwise, again with equal probability. For translational motion, signal dot direction could be either upwards or downwards on each trial with equal probability. Following previous studies (Burr & Santoro, 2001), the magnitude of the dot displacement was always constant across space in that it did not vary with distance from the origin as it would for strictly rigid global radial or rotational motion. This ensured that all stimuli were identical in terms of the speeds of the local dots. As such, performance for

radial and rotational motion could be directly compared to performance for translational motion.

Procedure

All measurements were carried out under either monocular or binocular viewing conditions. In the monocular viewing condition, measurements were taken with the sighting dominant eye. The other eye was occluded using an eye patch. In the binocular viewing condition, observers viewed the same stimulus but with both eyes. Motion coherence thresholds were measured using a single-interval, forced-choice, direction-discrimination procedure. On each trial observers were presented with an RDK stimulus. Performance was measured separately for each of the motion types and the order of testing was randomised. For radial motion, the task was to identify whether the global motion was expansion or contraction and for rotational motion, the task was to identify whether the dots rotated clockwise or anti-clockwise. For translational motion, the observers' task was to identify whether the global motion was upwards or downwards. Data-collection was carried out using a 3-down, 1-up adaptive staircase procedure (Edwards & Badcock, 1995) that varied the number of signal dots present on each trial, according to the observer's recent response history, to track the 79.4 % correct response level. At the beginning of each staircase all of the dots were assigned to be signal dots and the initial step size was set to be 8 signal dots. After each reversal the step size was halved, but the minimum step size was constrained to be 1 signal dot. The staircase terminated after eight reversals and the mean of the last six reversals was taken as the threshold estimate for that run of trials. Each observer completed 4 staircases for each condition and the mean threshold (expressed as the % of signal dots in the RDK) was calculated.

Results

Figure 2 shows motion coherence thresholds, averaged across all 6 observers, under monocular and binocular viewing conditions, plotted as a function of dot modulation depth separately for (a) radial, (b) rotational and (c) translational global motion, respectively. Results followed a broadly similar trend for all motion types

(radial, rotational & translational) in that motion coherence thresholds initially decreased as dot modulation depth increased, then changed relatively little with further increases in modulation depth. Thresholds were similar under monocular and binocular viewing conditions at all but the lowest modulation depths tested, where thresholds were somewhat higher when viewing was monocular. This suggests that the principle difference in performance between the two viewing conditions is characterised by a shift of the entire threshold versus modulation depth function primarily along the horizontal (modulation depth), rather than the vertical (motion sensitivity), axis.

<Insert Figure 2 about here>

To quantify the relationship between motion coherence thresholds and dot modulation depth the data were fit with the following equation, which we have used previously to characterise analogous functions obtained using first-order RDKs (Allen, Hutchinson, Ledgeway & Gayle, 2010):

$$y = \left[\frac{\left(\mathrm{sgn}\left(a - x\right)+1\right)\left(\frac{a}{x}\right)^{c} + \mathrm{sgn}\left(x - a\right)+1}{2} \right] b, \qquad [2]$$

where x is dot modulation depth and a, b and c are constants. Parameter a is the dot modulation depth above which performance on the task is no longer limited by the modulation depth and asymptotes at the motion coherence threshold b. Parameter c is the slope of the descending limb of the function (on log-log co-ordinates). Sgn(), or the signum function, is equal to either +1, 0 or -1 depending on whether the argument in parentheses is > 0, 0 or < 0, respectively.

Figure 3 shows the best fitting parameters derived from Equation 2 corresponding to the (a) dot modulation depths (parameter *a*) and (b) motion coherence thresholds

(parameter *b*) at which performance asymptoted (i.e. at the 'kneepoint')[1]. Figure 3 (c) shows derived monocular/binocular performance ratios for the modulation depth and motion parameters. These ratios characterise the magnitude of the horizontal shift, along the x-axis, and the vertical shift, along the y-axis, that would be needed to bring the two curves for each type of motion into correspondence. Slopes (parameter *c*) and R^2 values of the fit (Equation 2) are given in Table 1. It is evident that any binocular advantage for second-order global motion perception was driven primarily by enhanced sensitivity to modulations in stimulus contrast, rather than global motion processing *per se* (Figure 3c).

<Insert Figure 3 and Table 1 about here>

Figure 4 compares mean motion coherence thresholds for each motion type as a function of modulation depth under (a) monocular and (b) binocular viewing conditions. A 2 (viewing condition) by 3 (motion type) by 9 (modulation depth) within-groups analysis of variance (ANOVA) was performed using data from individual observers. Thresholds improved with higher modulation depths [$F(8,40)=62.970$; $p<0.001$] and binocular thresholds were lower than monocular thresholds [$F(1,5)=24.792$; $p<0.01$]. There was a significant main effect of motion type [$F(2,10)=5.035$; $p<0.05$]. Overall, thresholds for radial motion were higher than those for translational or rotational motion. There was a significant interaction between viewing condition and modulation depth [$F(8,40)=9.459$; $p<0.001$] reflecting that there were only differences between viewing conditions at lower modulation depths. There were also significant 2-way interactions between viewing condition and motion type [$F(2,10)=4.912$; $p<0.05$], and motion type and modulation depth [$F(16,80)=3.018$; $p<0.05$]. Previous studies (e.g. Aaen-Stockdale et al., 2007) have suggested that, with monocular viewing, sensitivity to radial second-order motion may be poorer than to rotational or translational second-order motion under some conditions.

[1] The standard error (SE) values shown in Figure 3 and Table 1 are those reported by the curve-fitting software *Prism* (GraphPad Software, Inc) used to estimate the best-fitting parameters of Equation 2. These are "asymptotic" or "approximate" standard errors of the parameters, as is also the case for virtually all other nonlinear regression programs (see Motulsky & Christopoulos, 2004). Further details can be found at http://www.graphpad.com/guides/prism/6/curve-fitting/index.htm?reg_how_standard_errors_are_comput.htm

To examine the effects of motion type in more detail, we performed separate, 2 (motion type) by 9 (modulation depth) ANOVAs to compare: (a) radial with rotational motion, (b) radial with translational motion and (c) rotational with translational motion under each of our two viewing conditions. The findings are shown in Table 2 where it is apparent that performance for discriminating the direction of radial motion was significantly worse than for rotational or translational motion, only under monocular viewing conditions. Performance for rotational and translational motion was equivalent (Figure 4; Table 2). These findings are in agreement with Aaen-Stockdale et al. (2007).

Finally, to parametrically examine the modulation depths at which performance under monocular viewing conditions deteriorated relative to performance under binocular viewing conditions, we performed separate 2 (viewing condition) by 9 (modulation depth) ANOVAs for each motion type. For radial motion, there were main effects of viewing condition [$F(1,5)=23.602$; $p<0.01$] and modulation depth [$F(8,40)=4.912$; $p<0.001$], and an interaction between the two factors [$F(8,40)=6.125$; $p<0.001$]. For rotational motion, there were main effects of viewing condition [$F(1,5)=8.646$; $p<0.05$] and modulation depth [$F(8,40)=31.32$; $p<0.001$], but no interaction between the two factors [$F(8,40)=1.464$; $p = .201$]. For translational motion, there were main effects of viewing condition [$F(1,5)=23.602$; $p<0.01$] and modulation depth [$F(8,40)=35.568$; $p<0.001$], and an interaction between the two factors [$F(8,40)=4.554$; $p<0.001$]. For each motion type, paired samples t-tests compared performance under monocular and binocular viewing conditions at each dot modulation depth. Results are given in Table 3 and were comparable across motion type. Sensitivity to translational global motion was most markedly affected by whether viewing was monocular or binocular in that motion coherence thresholds were significantly different at the greatest number of modulation depths. Rotational motion perception however was least affected by viewing condition, even at low dot modulation depths.

<Insert Figure 4 and Tables 2 & 3 about here>

Carrier visibility: To ensure that our findings were not due simply to monocular and binocular differences in the overall visibility of the static noise carrier, in a control experiment we measured carrier detection thresholds under monocular and binocular viewing conditions. Three observers (CH, AA, ML) performed a temporal two-alternative-forced-choice (2AFC) detection task, whereby they had to judge which of two temporal intervals (order randomised on each trial) contained an unmodulated, 2-d, static noise field. As in the global motion experiments outlined previously, the noise field was presented centrally within a circular display region subtending 12 ° in diameter. Detection thresholds (79.4 % correct) were measured using a 3-down, 1-up adaptive staircase. At the beginning of each staircase, the contrast of the noise field was set to a suprathreshold level (typically 6 dB above threshold based on pilot studies). After each reversal the step size was halved and the staircase terminated after 12 reversals. The mean of the last 4 reversals was taken as the detection threshold. Each observer completed 4 runs of trials (i.e. staircases) and a mean was taken. Figure 5 shows contrast detection thresholds for each observer under monocular and binocular viewing conditions. Although detection thresholds were lower (performance was better by a factor of 1.8 on average) under binocular, compared to monocular viewing conditions, thresholds under both viewing conditions were markedly below the contrast of the noise carrier employed in the RDK stimuli. As such, this confirms that the noise carrier used in the motion experiment was always suprathreshold and that its overall visibility was not the limiting factor affecting performance under monocular viewing. Furthermore any binocular summation of the carrier contrast between the two eyes cannot explain the pattern of results found, as it would be expected to affect both the dots and background equally leaving the effective contrast *difference* defining the dots unchanged.

<Insert Figure 5 about here>

Dioptric blur: Viewing a stimulus monocularly rather than binocularly potentially reduces its visibility by limiting the information available to the visual system. Reduced visual sensitivity can be empirically simulated by optical defocus. Positive dioptric blur, for example, spatially filters out higher spatial frequency information,

thereby effectively reducing the absolute contrast of the dots that make up the RDK. This technique has been employed previously to assess the effects of reducing dot contrast (modulation depth) on performance for judging the direction of first-order global motion (Simmers et al., 2003). In this case, the addition of dioptric blur of + 3 and 4 DS led to a lateral shift of the motion coherence threshold vs. modulation depth curve in that whilst performance at low first-order dot modulation depths was impaired under blurred viewing conditions, performance at higher dot modulation depths remained unaffected. To assess the effects of reducing the visible second-order dot modulation, we compared 3 observer's (AA, ML, CH) motion coherence thresholds for discriminating the direction of second-order radial, rotational and translational global motion under normal binocular viewing conditions and with the addition of dioptric blur at +3DS as a function of dot modulation depth. Figure 6 shows the effects of blur on mean motion coherence thresholds for each second-order motion type as a function of modulation depth. Performance is averaged across the 3 observers. For all second-order global motion types, the addition of +3DS blur led to a very marked lateral shift in the descending limb of the threshold vs. modulation depth functions along the abscissae towards higher modulation depths. However as the blurred data exhibit little, if any, evidence of clear asymptotic performance (i.e. a convincing 'knee-point') even at the highest modulation depths tested it is impossible to determine if there is also any appreciable vertical shift of the functions upwards. Equation 2 is ill-conditioned under these circumstances and provides poor fits to the data so no attempt was made to quantify the magnitude of these shifts. These findings are likely to reflect poor overall sensitivity of the visual system to second-order information, where modulation sensitivity is markedly lower for, and restricted to a much narrower range of spatial and temporal frequencies, for second-order compared to first-order motion (Hutchinson & Ledgeway, 2006). Indeed, in visual disorders known to produce deficits in contrast sensitivity, such as amblyopia, spatiotemporal windows of visibility for second-order motion are more restricted than for first-order motion. Moreover, within the visible range, amblyopes exhibit a more marked decrease in contrast sensitivity for second-order compared to first-order patterns. Indeed, in severely amblyopic individuals, some second-order motion cues are invisible (Simmers, Ledgeway, Hutchinson & Knox, 2011). One point worth noting is that reducing the absolute contrast of the second-order dots

using blur under binocular viewing conditions exceeded the effects of reducing the effective contrast of the dots by viewing RDKs under monocular, compared to binocular viewing conditions. The magnitude of the blur used was relatively high and severely attenuated the high spatial frequency components present in the noise carrier, that are critical for extracting the second-order image structure conveyed at coarser spatial scales. These findings may be relevant to studies of second-order motion perception in aging where marked contrast sensitivity deficits have been found for stationary and moving patterns (Tang & Zhou, 2009). Further studies using different amounts of optical defocus may provide key insights into how second-order signals are combined and, perhaps, how and/or why sensitivity to second-order information is characteristically different from sensitivity to first-order signals.

<Insert Figure 6 about here>

Comparison with first-order global motion: As a control to confirm the generality of the findings of Hess et al. (2007), we measured motion coherence thresholds for 2 observers (AA & ML) for determining the direction of radial, rotational and translational first-order global motion (luminance-defined dots) under monocular and binocular viewing. The principle difference between the first-order experimental conditions in this study and that of Hess et al. (2007) was the presence of a static noise carrier background in the present study. In Hess et al. (2007), dots were presented against a uniform ‘grey’ background.

All stimulus parameters were identical to those employed for second-order dots except that the modulation depth of the first-order dots was manipulated by increasing the mean luminance of the noise carrier within the dots relative to that of the noise carrier in the background region (c.f. Simmers et al., 2003). This was done using the following equation:

$$\text{Dot modulation depth} = (DL_{mean} - BL_{mean}) / (DL_{mean} + BL_{mean}), \qquad [3]$$

where DL_{mean} and BL_{mean} are the mean luminances of the carrier within the dots and background, respectively. Dot modulation varied in the range 0.0039-0.3. An example of a first-order dot field is shown in Figure 7.

<Insert Figure 7 about here>

Figure 8 shows mean motion coherence thresholds for the 2 observers (AA & ML) for determining the direction of radial, rotational and translational first-order global motion, as a function of dot modulation depth, under monocular and binocular viewing conditions. At relatively high modulation depths, motion coherence thresholds were similar under monocular and binocular viewing. At the lowest dot modulation depths however, thresholds were lower under binocular compared to monocular viewing conditions and the function describing the monocular results was shifted horizontally along the modulation depth (contrast) axis. Equation 2 was fit to each observer's data under each viewing condition, allowing the quantification of the relative effects of dot modulation depth (horizontal axis) and motion coherence threshold (vertical axis). The derived monocular/binocular performance ratios for the modulation depth and motion parameters are shown for each observer and each motion type in Figure 9. The magnitude of the modulation depth component shift required to align the binocular and monocular data was between ~ 1.5 and 2.3 (average = 1.78). These findings were in agreement with those shown previously by Hess et al. (2007) who found an average (across observers & motion type) monocular/binocular shift along the modulation depth axis of a factor of ~ 1.7.

<Insert Figures 8 & 9 about here>

Discussion

The findings of the present study have shown that discriminating the direction of second-order global motion under binocular viewing led to an improvement in performance by a factor of around 1.2 compared to monocular viewing. This binocular advantage was modulation depth dependent and did not represent a uniform improvement in global motion processing *per se*. This suggests that the site

of this binocular advantage is likely to be relatively early in the visual hierarchy, prior to the stage of global motion analysis, where the responses of neurons sensitive to second-order motion are known to exhibit a strong dependence on stimulus modulation depth (e.g. Ledgeway, Zhan, Johnson, Song & Baker, 2005). We arrived at a similar conclusion in a previous study using analogous first-order global motion stimuli, but in that case the magnitude of the binocular advantage (a factor of ~ 1.7) was much more pronounced (Hess et al., 2007). We have confirmed these findings for first-order global motion stimuli in the present study where we find that binocular advantage for luminance-modulated dots on a background of static noise to be in the region of 1.8 (Figures 8 & 9). Our current findings complement those in the spatial domain that have previously demonstrated that binocular summation is poorer for second-order, compared to first-order, stationary stimuli (e.g. Wong & Levi, 2005; Schofield & Georgeson, 2011). Taken together, these results suggest that weak binocular summation may be characteristic of mechanisms throughout the visual system that encode second-order stimulus attributes, i.e. in both the spatial and temporal domains.

There are a number of possible explanations for our current findings. One possibility is that there are markedly fewer binocular neurons sensitive to second-order image characteristics than to first-order properties, early in visual cortex. In this context, little binocular summation would occur because there would be little opportunity for the outputs of the two eyes to be combined. It may be the case for example that neurons that respond to second-order motion are predominantly monocular up to, and including, extrastriate visual cortex. There is evidence for monocular processing of second-order information in areas 17 and 18 of feline visual cortex (e.g. Zhou & Baker, 1994; 1996). However, binocular neurons have also been found for contrast-envelope stimuli in feline area 18 (Tanaka & Ohzawa, 2006). Furthermore, if second-order global motion processing were monocular in the early stages of visual processing, the monocular inputs would necessarily be combined in area V5/MT, where neurons exhibit a high degree of binocularity (e.g. Maunsell & van Essen, 1983). If this were the case, although we might expect little, or no more of a binocular advantage than (say) probability summation would predict along the modulation depth axis shown in Figure 2, our binocular versus monocular functions

would shift uniformly downwards on the y-axis signifying a binocular advantage in global motion processing (i.e. combination of monocular signals in V5/MT). This was not the case.

An alternative possibility is that second-order neurons are predominantly binocular throughout the motion pathway (i.e. driven well by both eyes). Psychophysically, there is markedly greater interocular transfer of second-order information than first-order information. This is the case for stationary (Whitaker, McGraw & Levi, 1997) and moving (Nishida, Ashida & Sato, 1994) patterns. From a neurophysiological perspective, first-order information requires relatively simple analysis based on linear processing of luminance variations across the receptive fields of V1 neurons. In the case of moving stimuli, outputs are combined in area V5/MT. Second-order information requires more complicated analysis and has typically been modeled as requiring a non-linear pre-processing stage consisting of a linear filter followed by a gross, pointwise nonlinearity such as rectification and a second stage of linear filtering, i.e. a filter-rectify-filter scheme. (Chubb & Sperling, 1988; Wilson et al., 1992; Sutter, Sperling & Chubb, 1995). It has been proposed that initial filtering and rectification occurs in area V1, after which the rectified output is sent to area V2 for a second stage of filtering. The output of V2 is then sent to area V5/MT (e.g. Wilson et al., 1992). In the context of our present findings, the role of V2 in second-order motion processing is important because the majority of neurons in this area are binocularly driven (e.g. Zeki, 1978).

Irrespective of the precise nature of the underlying summation mechanisms, a critical feature of the current results concerns the magnitude of the binocular advantage found for global second-order motion patterns at low modulation depths. The binocular improvement in modulation depth sensitivity (a factor of ~ 1.2) was considerably less than that found previously for analogous first-order RDKs and also for the simple carrier detection task (see Figure 5) of the present study. This relatively weak binocular enhancement for second-order stimuli is smaller than would be expected by either simple probability summation across monocular inputs or neural (linear) summation arising from the convergence of monocular information into binocular motion-sensitive pathways. In both cases conventional models would

predict that binocular viewing should enhance sensitivity to modulations in stimulus contrast by at least a factor of 1.4 (e.g. Pirenne, 1943; Campbell & Green, 1965; Legge, 1984). Of course this prediction is critically dependent on the underlying assumption that the *internal* noise associated with the two monocular inputs are entirely independent. Although this may not be an unreasonable assumption in the case of global first-order motion perception, the present results strongly suggest that it may be invalid for the pathways that encode global second-order motion. Previous research has highlighted that even a weak correlation in the noise inherent in different visual neurons can severely limit the statistical benefits of summating their outputs (Zohary, Shadlen & Newsome, 1994). Future electrophysiological investigations exploring the covariation in firing rate of pairs of monocular neurones sensitive to second-order motion, to repeated presentations of the same stimulus, are needed to address this interesting possibility.

References

Aaen-Stockdale, C., Ledgeway, T. & Hess, R.F. (2007). Second-order optic flow processing. *Vision Research*, 47(13), 1798-808.

Andersen, R. A. (1997). Neural mechanisms of visual motion perception in primates. *Neuron*, 18, 865-872.

Albrecht, D.H. & Hamilton, D.B. (1982). Striate cortex of monkey and cat: Contrast response function. *Journal of Neurophysiology*, 48, 217-237.

Albright, T.D. (1987). Isoluminant motion processing in macaque visual area MT. *Society for Neuroscience Abstracts*, 13, 1626.

Albright, T.D. (1992). Form-cue invariant motion processing in primate visual cortex. *Science,* 255, 1141-1143.

Albright, T.D. (1993). Cortical processing of visual motion. In F.A. Miles & J. Wallman, Visual Motion and its Role in the Stabilisation of Gaze. Elsevier: Amsterdam.

Allen, H. A., Hutchinson, C. V., Ledgeway, T., & Gayle, P. (2010). The role of contrast sensitivity in global motion processing deficits in the elderly. *Journal of Vision*, 10(10):15, 1–10, http://www.journalofvision.org/content/10/10/15, doi:10.1167/10.10.15.

Ashida, H., Lingnau, A., Wall, M.B. & Smith, A.T. (2007). fMRI adaptation reveals separate mechanisms for first- and second-order motion. *Journal of Neurophysiology*, 97, 1319-1325.

Badcock, D.R. & Khuu, S.K. (2001). Independent first- and second-order motion energy analyses of optic flow. *Psychological Research,* 65, 50-56.

Baker, C.L. Jr. (1999). Central neural mechanisms for detecting second-order motion. *Current Opinion in Neurobiology*, 9, 461-466.

Burr, D. C. & Santoro, L. (2001). Temporal integration of optic flow, measured by contrast and coherence thresholds. *Vision Research* 41, 1891-1899.

Campbell, F.W. & Green, D.G. (1965). Monocular versus binocular visual acuity. *Nature,* 191-192.

Chaudhuri, A., & Albright, T.D. (1997). Neuronal responses to edges defined by luminance vs. temporal texture in macaque area V1. *Visual Neuroscience* 14, 949-962.

Chubb, C. & Sperling, G. (1988). Drift-balanced random stimuli: A general basis for studying non-Fourier motion perception. *Journal of the Optical Society of America A*, 5, 1986-2007.

Churan, J.& Ilg, U.J. (2001). Processing of second-order motion stimuli in primate middle temporal area and medial superior temporal area. *Journal of the Optical Society of America A*, 18, 2297-2306.

Duffy, C.J. & Wurtz, R.H. (1991). Sensitivity of MST neurons to optic flow stimuli I. A continuum of response selectivity to large-field stimuli. *Journal of Neurophysiology,* 65, 1329-1345.

Dumoulin, S.O., Baker, C.L., Hess, R.F. & Evans, A.C. (2003). Cortical specialisation for processing first- and second-order motion. *Cerebral Cortex*, 13, 1375-1385.

Dürsteler, M.R. & Wurtz, R.H. (1988). Pursuit and optokinetic deficits following chemical lesions to cortical areas MT and MST. *Journal of Neurophysiology*, 60, 940-965.

Edwards, M. & Badcock, D. (1995). Global motion perception: No interaction between the first- and second-order pathways. *Vision Research*, 35, 2589-2602.

Geesaman, B.J. & Anderson, R.A. (1996). The analysis of complex motion patterns by form/cue invariant MSTd neurons. *Journal of Neuroscience* 16, 4716-4732.

Giaschi, D. E., Regan, D., Kraft, S. P. & Hong, X. H. (1992). Defective processing of motion-defined form in the fellow eye of patients with unilateral amblyopia. *Investigative Ophthalmology & Visual Science*, 33, 2483–2489.

Greenlee, M. W., & Smith, A. T. (1997). Detection and discrimination of first- and second-order motion in patients with unilateral brain damage. *The Journal of Neuroscience*, 17, 804-818.

Greenwood, J. A., & Edwards, M. (2006). Pushing the limits of transparent-motion detection with binocular disparity. *Vision Research*, 46(16), 2615-2624.

Grossberg, S., Mingolla, E. & Pack, C. (1999). A neural model for motion processing and visual navigation by cortical area MST. *Cerebral Cortex*, 9, 878-895.

Hall, S. D., Holliday, I. E., Hillebrand, A., Furlong, P. L., Singh, K. D. & Barnes, G. R. (2005). Distinct contrast responses functions in striate and extrastriate regions of visual cortex revealed with magnetoencephalography. *Clinical Neurophysiology*, 116, 1716-1722.

Hess, R.F., Hutchinson, C.V., Ledgeway, T. & Mansouri, B. (2007). Binocular influences on global motion processing in the human visual system. *Vision Research*, 47, 1682-1692.

Hutchinson, C.V. and Ledgeway, T. (2006). Sensitivity to spatial and temporal modulations of first-order and second-order motion. *Vision Research*, 46, 324-335.

Hibbard, P. B. & Bradshaw, M. F. (1999). Does binocular disparity facilitate the detection of transparent motion? *Perception*, 28(2), 183–191.

Ledgeway, T., Zhan, C., Johnson, A., Song, Y. & Baker, C.L. Jr. (2005). The direction-selective contrast response of area 18 neurons is different for first- and second-order motion. *Visual Neuroscience*, 22, 87-99.

Ledgeway, T. & Smith, A.T. (1994). Evidence for separate motion-detecting mechanisms for first- and second-order motion in human vision. *Vision Research*, 34, 2727-2740.

Legge, G.E. (1984). Binocular contrast summation – II. Quadratic summation. *Vision Research*, 24, 385-394.

Lu, Z-L., & Sperling, G. (2001). Three-systems theory of human visual motion perception: review and update. *Journal of the Optical Society of America A,* 18, 2331-2370.

Livingstone, M.S., Pack, C.C. & Born, R.T. (2001). Two-dimensional substructure of MT receptive fields. *Neuron*, 30, 781-793.

Mather, G. & Murdoch, L (1998). Evidence for global motion interactions between first-order and second-order stimuli. *Perception*, 27, 761-767.

Maunsell, J. H. R. & van Essen, D. C. (1983). Functional properties of neurons in the middle temporal visual area (MT) of the macaque monkey: Selectivity for stimulus direction, speed and orientation. *Journal of Neurophysiology*, 49, 1127-1147.

Motulsky, H. & Christopoulos, A. (2004). *Fitting models to biological data using linear and non-linear regression: a practical guide to curve fitting.* Oxford: Oxford University Press.

Movshon, J.A. & Newsome, W.T. (1996). Visual response properties of striate cortical neurons projecting to area MT in macaque monkeys. *Journal of Neuroscience*, 16, 7733-7741.

Newsome, W.T. & Paré, E.B (1988). A selective impairment of motion perception following lesions of the middle temporal visual area (MT). *Journal of Neuroscience*, 8, 2201-2211.

Nishida, S., Ashida, H. & Sato, T. (1994). Complete interocular transfer of motion aftereffect with flickering test. *Vision Research*, 34, 2707-2716.

Nishida, S., Sasaki, Y., Murakami, I., Watanabe, T. & Tootell, R.B.H. (2003). Neuroimaging of direction-selective mechanisms for second-order motion. *Journal of Neurophysiology*, 90, 3242-3254.

Pirenne, M. H. (1943). Binocular and uniocular threshold of vision. *Nature*, 152, 698.

Schiller, P. H. (1993). The effects of V4 and middle temporal (MT) area lesions on visual performance in the rhesus monkey. *Visual Neuroscience*, 10, 717-746.

Schofield, A.J. & Georgeson, M.A. (2011). Functional architecture for binocular summation of luminance- and contrast-modulated gratings. *Perception (Supplement)*, 40, 17.

Seifert, A.E., Somers, D.C., Dale, A.M. & Tootell, R.B.H. (2003). Functional MRI studies of human visual motion perception: texture, luminance, attention and after-effects. *Cerebral Cortex*, 13, 340-349.

Simmers, A. J., Ledgeway, T., Hess, R. F., & McGraw, P. V. (2003). Deficits to global motion processing in human amblyopia. *Vision Research*, 43, 729–738.

Simmers, A. J., Ledgeway, T., Hutchinson, C.V. & Knox, P.J. (2011). Visual deficits in amblyopia constrain normal models of second-order motion processing. *Vision Research*, 51, 2008-2020.

Snowden, R.J. & Rossiter, M.C. (1999). Stereoscopic depth cues can segment motion information. *Perception*, 28(2), 193–201.

Stoner, G.R. & Albright, T.D. (1992). Motion coherency rules are form-cue invariant. *Vision Research*, 32, 465-475.

Sutter, A., Sperling, G. & Chubb, C. (1995). Measuring the spatial frequency selectivity of second-order texture mechanisms. *Vision Research*, 35, 915-924.

Tanaka, H. & Ohzawa, I. (2006). Neural basis for stereopsis from second-order contrast cues. *Journal of Neuroscience*, 26: 4370-4382.

Tang, Y. and Zhou, Y-F. (2009). Age-related decline of contrast sensitivity for second-order stimuli: Earlier onset but slower progression, than for first-order stimuli. *Journal of Vision,* 9(7):18, 1-15.

Vaina, L.M. & Soloviev, S. (2004). First-order and second-order motion: neurological evidence for neuroanatomically distinct systems. *Progress in Brain Research,* 144, 197-212.

Whitaker, D., McGraw, P. V., & Levi, D. M. (1997). The influence of adaptation on perceived visual location. *Vision Research*, 37, 2207–2216.

Wilson, H.R., Ferrera, V.P. & Yo, V. (1992). Psychophysically motivated model for two-dimensional motion perception. *Visual Neuroscience*, 9, 79-97.

Wong, E.H. & Levi, D.M. (2005). Reduced binocular summation of second-order contrast in amblyopia. *Investigative Ophthalmology and Visual Science (Supplement)*, 46, 5645.

Zeki, S. (1978). Functional specialization in the visual cortex of the rhesus monkey. *Nature*, 274, 423–428.

Zohary, E., Shadlen, M.N. & Newsome, W.T. (1994). Correlated neuronal discharge rate and its implications psychophysical performance. *Nature*, 370, 140-143.

Zhou, Y.X. & Baker, C.L. Jr. (1993). A processing stream in mammalian visual cortex neurons for non-Fourier responses. *Science*, 261, 98-101.

Zhou, Y.X. & Baker, C.L. Jr. (1994). Envelope-responsive neurons in area 17 and 18 of cat. *Journal of Neurophysiology*, 72, 2134-2150.

Figures

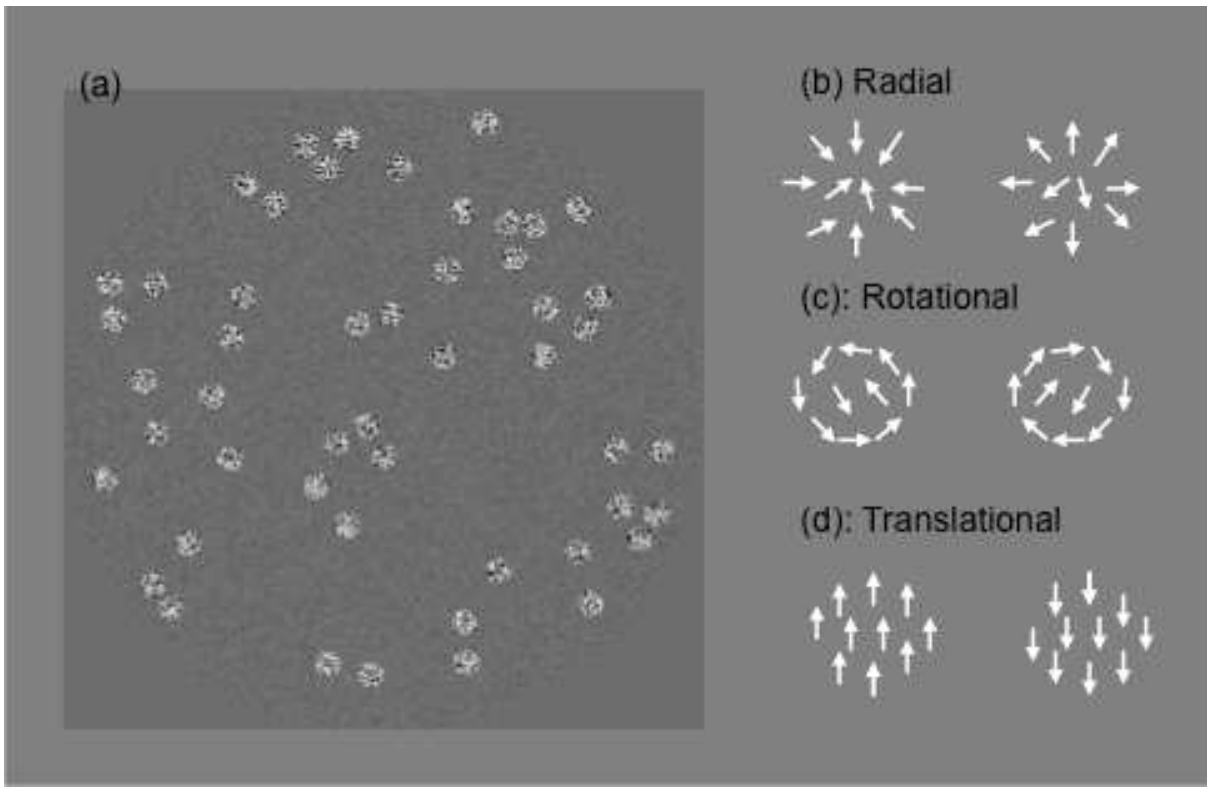

Figure 1. (a) Example of a second-order (contrast defined) dot field and depictions of (b) radial (contraction vs. expansion), (c) rotational (anti-clockwise vs. clockwise) and (d) translational (upwards vs. downwards) motion signal dot trajectories.

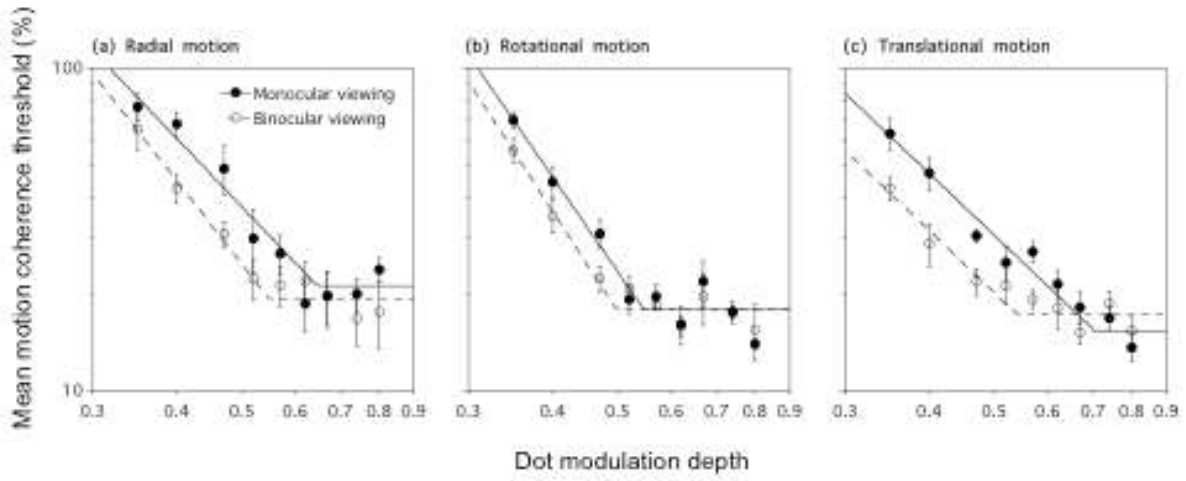

Figure 2. Mean global motion coherence thresholds for identifying the direction of (a) radial, (b) rotational and (c) translational second-order global motion as a function of dot modulation depth (contrast) under monocular (open circles) and binocular (closed circles) viewing conditions. Data have been fit with Equation 2. The point at which the two limbs of the function intersect represent parameters *a* (dot modulation depth – x axis) and *b* (motion coherence threshold – y axis) of Equation 2. Error bars represent ± 1 S.E.M.

Figure 3

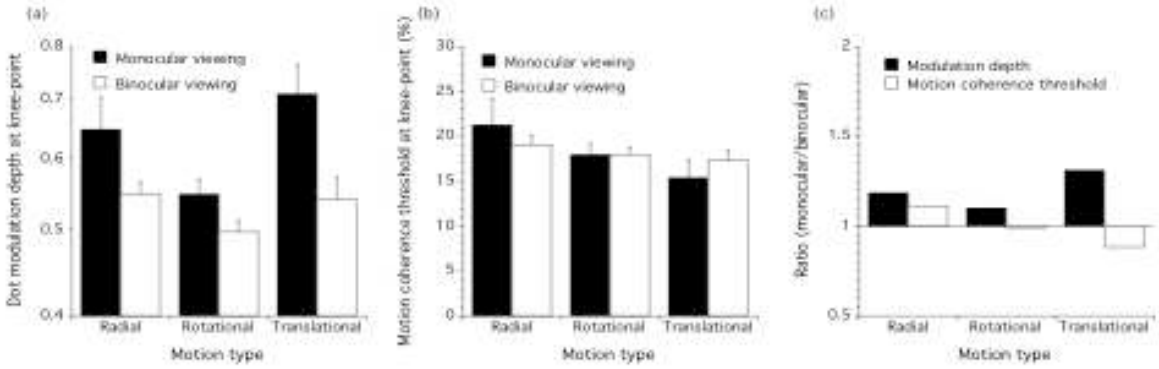

Figure 3. (a) Dot modulation depths and (b) motion coherence thresholds at the 'knee-point' derived from fitting Equation 2 to the data for each motion type (radial, rotational & translational) under each viewing condition (monocular & binocular). (c) Derived monocular/ binocular performance ratios of the best fitting parameters describing the lateral (modulation depth: Figure 3a) and vertical (motion sensitivity: Figure 3b) shifts needed to bring the monocular and binocular motion coherence threshold versus modulation depth functions into correspondence.

Figure 4

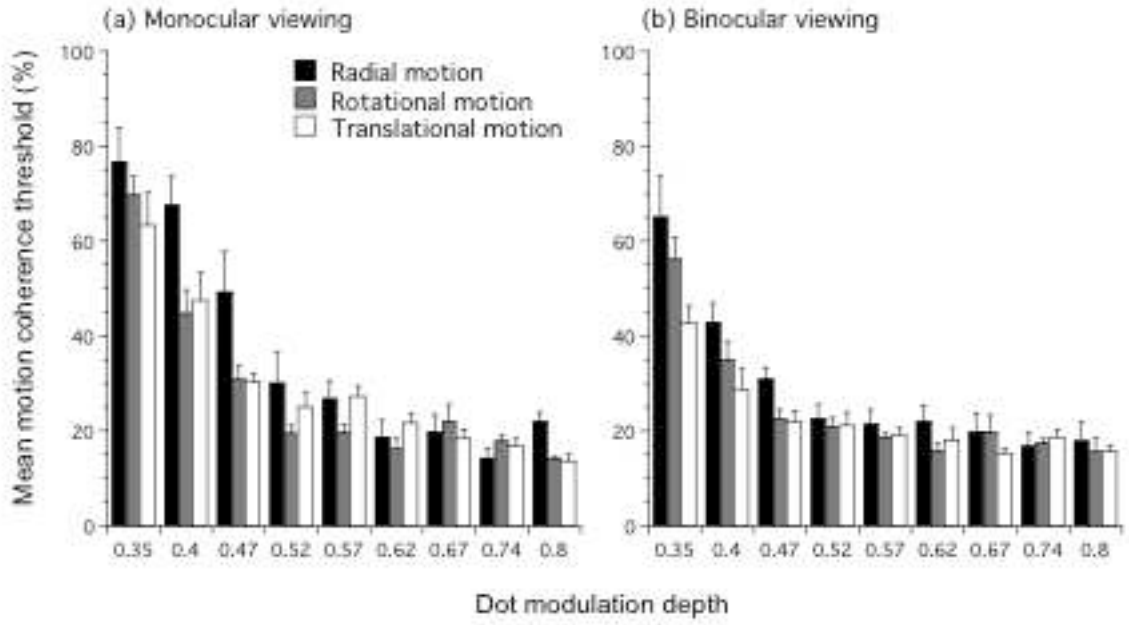

Figure 4. Mean motion coherence thresholds for each motion type at each dot modulation depth under (a) monocular and (b) binocular viewing conditions. Error bars represent ± 1 S.E.M.

Figure 5

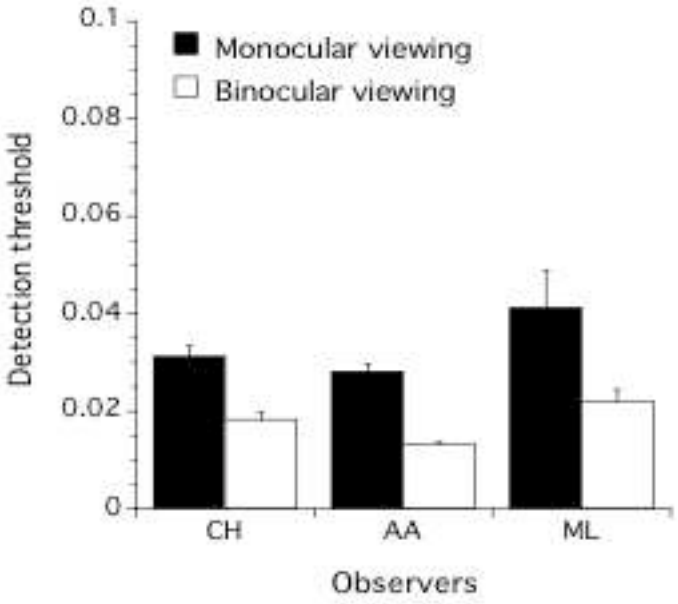

Figure 5. Contrast thresholds for 3 observers for detecting the presence of the 2-d noise carrier under monocular and binocular viewing conditions. Error bars are ± 1 S.E.M.

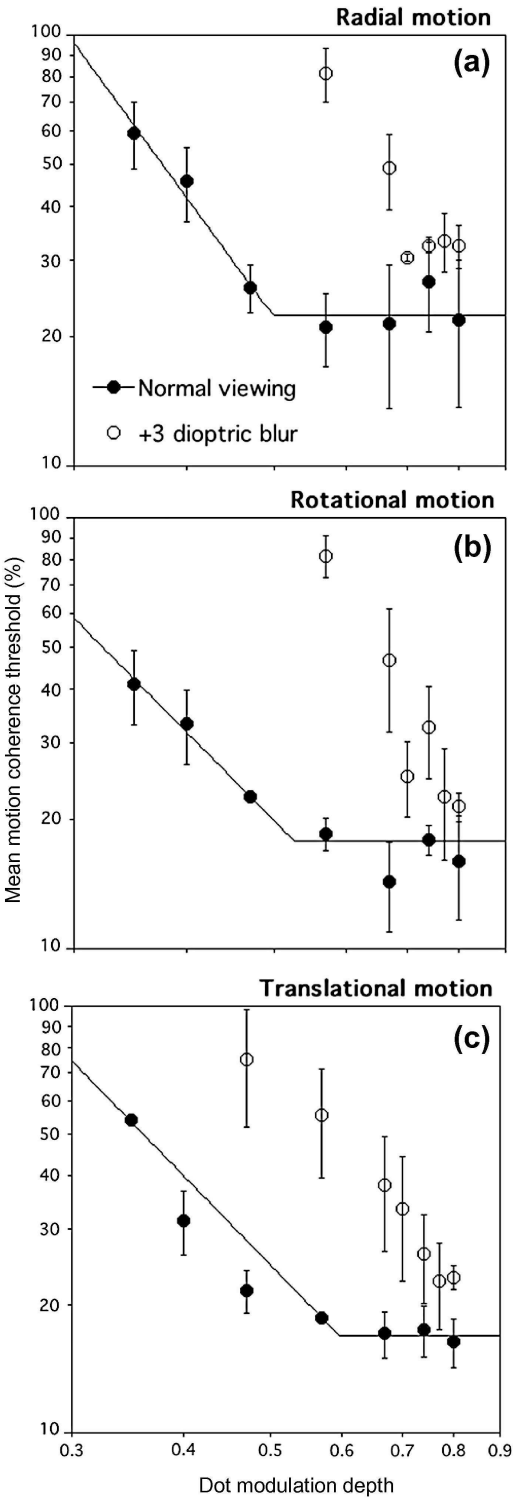

Figure 6. Mean global motion coherence thresholds for identifying the direction of (a) radial, (b) rotational and (c) translational second-order global motion as a function of dot modulation depth under normal, in-focus, binocular viewing conditions and with +3 dioptre blur. The unblurred binocular data have been fit with Equation 2 and are represented by the solid line in each plot. The averaged data under blurred binocular viewing conditions exhibit considerable variability and little evidence of asymptotic performance (i.e. a convincing 'knee-point') even at the highest modulation depths tested and therefore were not fitted with Equation 2 (see text for further details). Error bars represent ± 1 S.E.M.

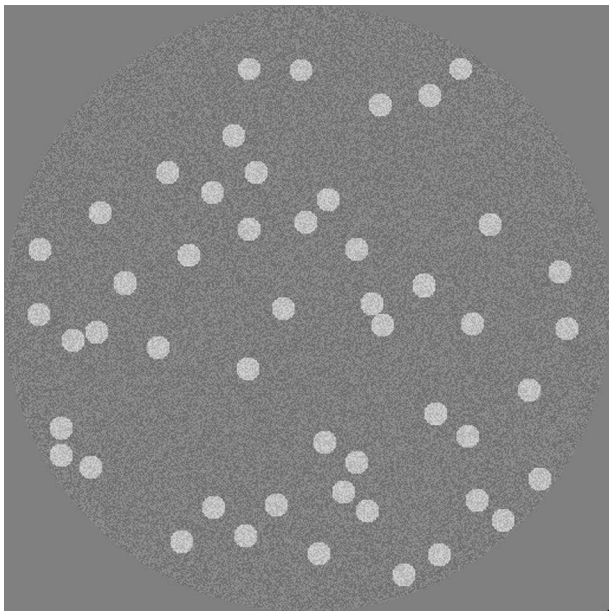

Figure 7. Example of a first-order (luminance defined) dot field (see Equation 3).

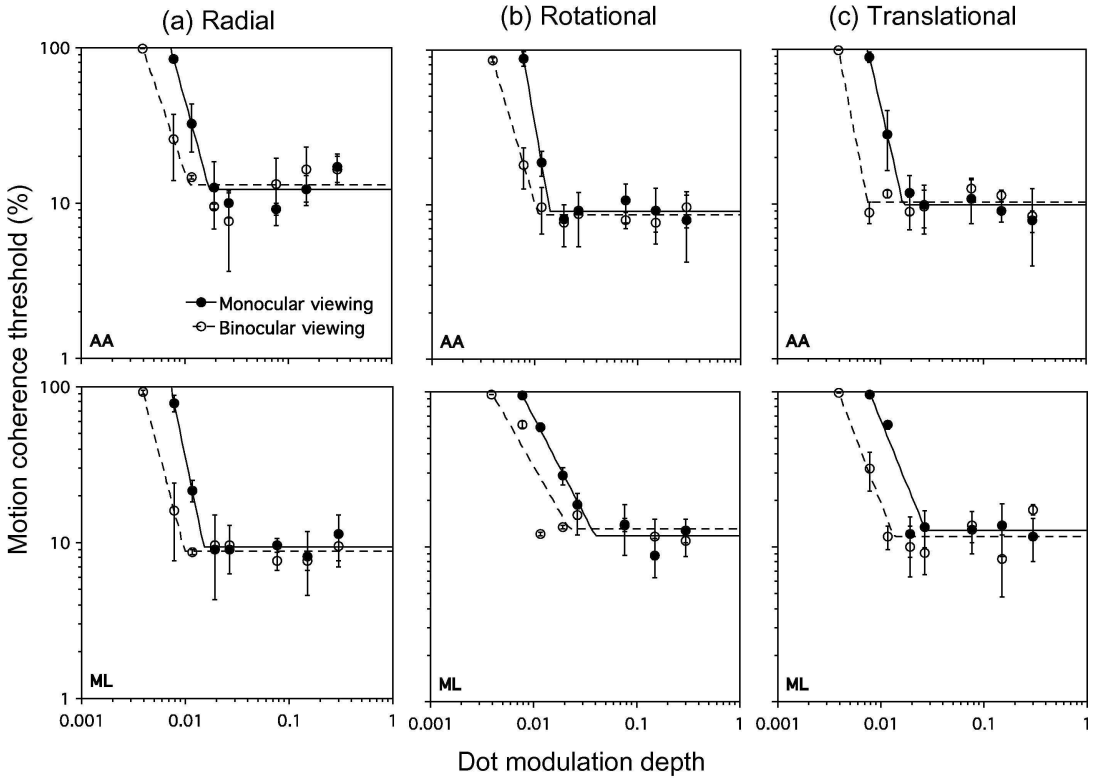

Figure 8. Comparison of mean global motion coherence thresholds for 2 observers for identifying the direction of (a) radial, (b) rotational and (c) translational first-order global motion as a function of dot modulation depth (contrast) under monocular and binocular viewing conditions. Data have been fit with Equation 2. Error bars represent ± 1 S.E.M.

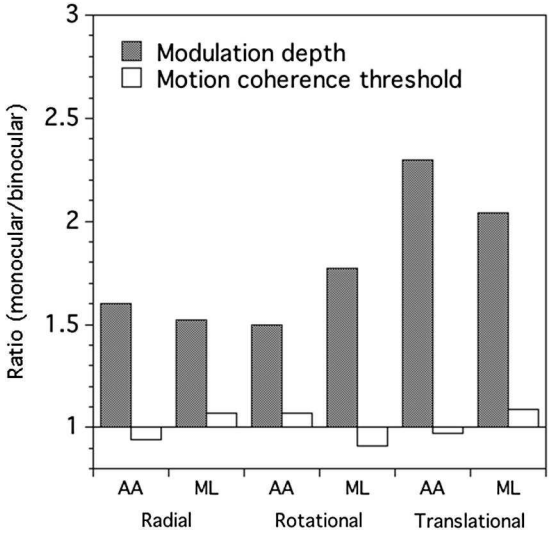

Figure 9. Derived monocular/binocular performance ratios of the best fitting parameters describing the lateral and vertical shifts needed to bring the monocular and binocular motion coherence threshold versus modulation depth functions into correspondence.